Appl Compos Mater (2013) 20:489–503
DOI 10.1007/s10443-012-9283-6

Acoustic Emission as a Tool for Damage Identification and Characterization in Glass Reinforced Cross Ply Laminates

D. G. Aggelis · N.-M. Barkoula · T. E. Matikas · A. S. Paipetis

Received: 5 March 2012 / Accepted: 13 July 2012 / Published online: 31 July 2012

Abstract Loading of cross-ply laminates leads to the activation of distinct damage mechanisms, such as matrix cracking, delaminations between successive plies and fibre rupture at the final stage of loading. This study deals with the investigation of the failure of cross ply composites by acoustic emission (AE). Broadband AE sensors monitor the elastic waves originating from different sources of failure in coupons of this material during a tensile loading-unloading test. The cumulative number of AE activity, and other qualitative indices based on the waveforms shape, were well correlated to the sustained load and mechanical degradation as expressed by the gradual decrease of elastic modulus. AE parameters indicate the succession of failure mechanisms within the composite as the load increases. The proposed methodology based on Acoustic Emission for the identification of the damage stage of glass reinforced cross ply laminates is an initial step which may provide insight for the study of more complex laminations.

Keywords Acoustic emission · Composite materials · Cross ply laminates · Damage monitoring · Failure modes

1 Introduction

Real time characterization of the structural condition of composite laminates is a demanding task. These materials suffer deterioration owing to different mechanisms, such as matrix cracking, delamination between successive plies and fibre rupture at the final stage of loading, with extensive fibre pull out. A suitable model composite material configuration to study different failure mechanisms and their interaction is the cross-ply laminate. In cross ply laminates, deterioration starts by tensile matrix cracks in the plies with fibres perpendicular to the loading direction [1–3]. At the location of the cracks, and depending on the interlaminar shear strength, stress concentration triggers delaminations between the off- and on-loading axis plies, or longitudinal fibre cracks. Matrix cracking is led to a saturation level

D. G. Aggelis · N.-M. Barkoula · T. E. Matikas · A. S. Paipetis (✉)
Department of Materials Science and Engineering, University of Ioannina, Ioannina 45110, Greece
e-mail: paipetis@cc.uoi.gr

usually well before final failure, and thereafter delaminations and cumulative fibre failure at the 0° ply become dominant until catastrophic failure. Matrix cracking is indispensable for the creation of the shear discontinuity that will trigger all other mechanisms that follow. However, it is certain that after the first transverse matrix cracks and before saturation, these cracks develop simultaneously with delaminations and longitudinal fibre breaks in an overlapping period. A good knowledge of the initiation and propagation of damage related to the applied load, enables optimization of the interfacial properties resulting in longer durability which is the final engineering goal [4].

Acoustic emission has been used for monitoring of the structural health and damage accumulation for different types of materials [5–7]. Composite materials are of particularly interest for AE monitoring, as the multiplicity and interdependence of failure modes may be traced in the acoustic signature of the tested material [8–10]. The AE activity rate together with other qualitative parameters of the incoming signals provides insight in the fracture pattern. In general, the information from AE concerns the location of damage, as well as the severity based on the rate of the received AE signals. When one crack propagation incident occurs, the emitted waves are acquired almost simultaneously by the different sensors. The time delay between the acquisition of the signals at the different measurement points leads to the calculation of the "event" location [11–13]. The event corresponds to the fracture incident while the emitted wave may be received by a number of sensors depending on their distance from the source and material attenuation as distinct "hits". In this way, the exact location of each specific crack can be determined and areas concentrating high damage content are characterized, information which is very important for the case of actual size structures and enables the proper repair action. Additionally the number of acquired signals is indicative of the number of cracks, since the source of AE is cracking. Low activity is correlated to few source cracks, while high AE rate underlines the existence of numerous cracks. As should be noted at this point, location is related to the solution of the inverse problem of wave propagation from a point source. For isotropic plates, the problem relates to the "triangulation" of the emitted signal [14]. Although plate waves are by nature dispersive, in this simple case and for low frequencies the location is sufficiently accurate by regarding the waves as non dispersive [15]. However, there is increasing complexity when anisotropy is introduced as in the case of composite laminates which renders the isotropic solution redundant and requires more advanced techniques [16, 17]. The location problem is further complicated for complex geometries, where array signal processing must be combined with the dispersive nature of plate waves [18].

Apart from the above pieces of valuable information, additional insight to the cracking process can be provided by qualitative aspects of the AE waves. In the case of macroscopically isotropic materials such as fibre reinforced concrete [19], the shape of the acquired waveforms can be correlated to the fracture mode. The two basic modes (tensile and shear) include different relative direction of motion between the crack sides. This leads to different wave types emitted, and therefore, to different signature waveforms [20]. In general, tensile cracks, due to the emission of longitudinal waves result in short waveforms, with short rise time and therefore, high rise angle, as seen in Fig. 1. On the contrary, mode II cracks, emit more energy in the form of shear waves which are slower resulting in a longer rise rime (RT), and consequently lower rise angle [19]. In this case as has been extensively reported in the literature [21–24], the frequency emitted by tensile cracks is higher than shear in bulk materials. Therefore, monitoring of the qualitative characteristics of the waveforms supplies real time information on the different cracking modes. It is however obvious that in the case of anisotropic composite laminates the problem becomes much more complicated and requires in depth knowledge of the interconnected mechanisms that trigger and accumulate

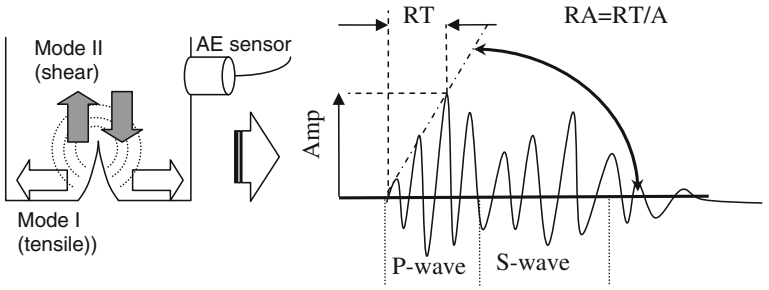

Fig. 1 Acoustic emission incident and typical waveform recorded by the sensor

damage. Particularly for cross-ply laminates shear fracture (delaminations) follows tensile (matrix cracking) and thus classification of cracks may lead to evaluation of the current damage status and an early warning prior to final failure [25, 26]. For the sake of completeness, it is mentioned that the waveform detected by the sensors may substantially differ from the emitted wave. This is reasonable due to propagation of distinct modes with different velocity, scattering on inhomogeneities, as well as geometric constrains which are certainly active in the case of plates, rendering propagation dispersive [27]. Therefore, the interpretation of the qualitative features of the signals is a demanding task which should mainly be based on the relative change of waveforms, which is certainly setting a limitation for monitoring large structures. On the other hand, the identification of specific modes of the original waveform from the detected waveform may be feasible in simple well defined systems [28] but would be extremely complicated in the case of composite materials. In this case the microstructure, the geometry, the multiplicity /interconnection of damage mechanisms which affect the propagates signal are extremely complex, particularly in relation to damage location [29]. In the case of all cross ply composite coupons for this study, (i) the geometry of the specimens and the measuring system were constant, (ii) the positioning of the sensors was defined and (iii) propagation was monitored along a linear trajectory. In this respect, it could be assumed that any shift of the values of the AE parameters during the experiment may be safely attributed to the irreversible changes due to damage within the small gauge length.

Although pattern recognition techniques have been extensively employed to correlate the structural state of the composite to its acoustic activity [26, 30], this work aims in correlating specific signal attributes to the damage state of the glass reinforced cross ply laminates. In a previous study, optically transparent glass fibre reinforced cross ply laminates were loaded in tension allowing for the concurrent observation of the transverse cracking process and the subsequent triggering of distinct damage mechanisms [30]. Using unsupervised pattern recognition mechanisms, the AE activity of the loaded coupons was classified and attributed to specific damage mechanisms. Within the scope of this work, cross-ply glass/epoxy coupons are subjected to incremental triangular step loading until failure with simultaneous acoustic emission monitoring. Multiple AE parameters like the total activity, waveform shape parameters and indices exhibit distinct trends and are correlated to the sustained load and the stiffness loss as manifested by the reduction of the Young's modulus for consecutive loading cycles. It is suggested that AE monitoring can promote the understanding on the accumulation of damage as manifested by the succession of distinct fracture processes in the material and provide real time characterization of the structural integrity of the composite laminate.

2 Experimental Details

The cross-ply laminates were fabricated by hand layup with a sequence $[0°_4/90°_4]$ s, resulting in a total number of 16 plies with total specimen thickness of 4 mm. The unidirectional 220 g/m2 (Aero) unidirectional glass fibre fabric was impregnated using the HT2 epoxy resin/ hardener matrix system (mixing ratio 100:48) manufactured by R&G Faserverbundwerkstoffe GmbH Composite Technology. A 250×250 mm^2 laminate was manufactured and was allowed to cure for 24 h at room temperature. Tensile specimens were subsequently cut according to the ASTM D3039 standard, at a length of 100 mm and a width of 20 mm, as specified in ASTMD3039 for composites of other than unidirectional geometry. End tabs cut from the same laminate were glued to all specimens prior to testing so as to avoid failure due to stress concentrations at the hydraulic grips of the tensile loading frame.

The specimens were loaded in load controlled tension, in a step loading mode. A photograph of the experiment is seen in Fig. 2a. The loading consisted of a saw-tooth spectrum formed from a sequence of triangular loading / unloading steps see Fig. 2b. A rate 5 kN/min was employed for both loading and unloading, so as to comply with the requirements of 1–10 min duration from zero load to ultimate failure at the last loading cycle. The maximum load was incremented by 4 kN at each consecutive step. The step loading continued until the tensile failure of the specimen. All tensile tests were performed using an Instron Universal Testing Machine equipped with hydraulic gripping system, under load control, at controlled environmental conditions of 25 °C and 70 % relative humidity. The elastic modulus measurements for each consecutive step were performed according to the ASTM D3039 Standard Test Method for Tensile Properties of Polymer Matrix Composite Materials for the calculation of the chord modulus, employing a strain range corresponding to 25–50 % of ultimate load for each consecutive cycle and of the failure load for the last loading cycle. The chord modulus of elasticity, thereafter referred to as modulus of Elasticity was calculated as $E=\Delta\sigma/\Delta\varepsilon$. A total of three specimens were employed for this study and all presented data refer to cumulative data collected from all three specimens.

For the purpose of the AE monitoring, two wide band AE sensors (Pico, Physical Acoustics Corp., PAC) were attached on the same side of the specimen (Fig. 2a). Electron wax was applied between the sensors and the specimen to provide acoustic coupling, while it offered the necessary support to the sensors during the experiment. The specific sensors were chosen over other AE transducers mainly due to their spectral response. They are sensitive to frequencies from 100 kHz up to approximately 800 kHz, with maximum sensitivity at 500 kHz. Therefore, they can capture a wide range of different sources. According to the calibration sheet provided by the manufacturer, the response between 300 kHz and 600 kHz is within a range of 3 dB. Details about the employed sensors may be found in [31]. The frequency content of the typical acoustic emission activity of material systems such as employed in this study was well within the window of the sensitivity of the employed sensors [32, 33]. The distance between the two receivers was set at 70 mm.

The pre-amplifier gain was set to 40 dB. After performing a pilot test, the threshold was also set to 40 dB, in order to avoid electronic/environmental noise. The signals were recorded employing a two-channel PCI-2 monitoring board of PAC with sampling rate of 5 MHz. The sampling rate was an order of magnitude higher than the central frequencies of the acquired AE hits. Within the purposes of this study, significant relative changes of the acoustic activity with step loading were

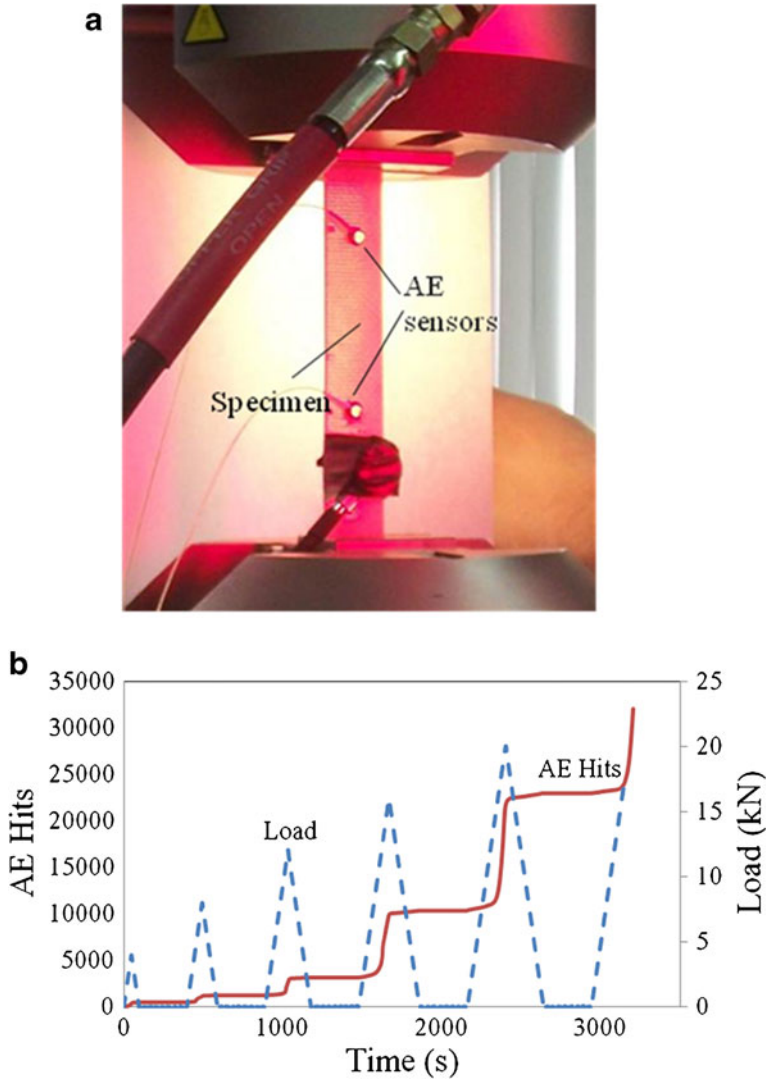

Fig. 2 **a** Experimental setup, **b** Typical Load & AE activity vs. Time for the specimens tested

identified and evaluated within the sensitivity of the sensors and sampling rate capability of the acquisition board. As the acquisition system was limited to two channels, there was no possibility to definitely exclude all emanating Acoustic Activity from the loading frames or the grips, e.g. by the use of coincidence detectors. However, since (i) no acoustic emission activity was recorded after the gripping and prior to loading and (ii) the recording of "events" within the monitored length (Fig. 2a) revealed the same trends as the entire data set, it was assumed that acoustic activity other that related to specimen damage was not significant. For the purposes of this study, the hit lock out time was specified at its maximum allowable value (65 ms). This resulted to a maximum recording rate of approximately 400 hits/s at the moments of intense acoustic activity.

3 Results and Discussion

Acoustic emission can provide information on different levels. One is the correlation of parameters measured nondestructively with mechanical data of sustained load or elastic modulus degradation since acoustic emission activity is the result of damage accumulation. This damage accumulation may be of different origin, (i.e. matrix cracking and/or delaminations and/or fibrerupture), according to the loading conditions. Even if there is no insight on the actual mechanism, damage increases with load and is the reason for material degradation. Stiffness loss is the most indisputable measure of structural degradation and as AE activity is emitted during damage accumulation, it is expected to correlate well to the macroscopic readings of elastic modulus or sustained load. As will be seen, the proper study of observed correlations enables the estimation of macroscopic parameters based on a simple AE monitoring. The study of these correlations may enhance the understanding of the failure process and promote its early prognosis, which is one of the final goals of the approach. Additionally, as mentioned in the Section 1, some AE indices offer insight on the specific active fracture mechanisms and can be used for better understanding of the process.

As can be seen in Fig. 2b, the AE activity increased progressively for each successive load step from a few hundred hits at the first step to more than 10,000 for the last step. From the line of cumulative hits, it is suggested that as the load steps succeed each other, the AE activity is more intense, something reasonable due to the damage accumulation that creates new active sources. In a typical experiment employing the aforementioned loading protocol, approximately 40,000 hits are recorded until the catastrophic failure of the composite coupon.

3.1 Phenomenological Correlations

As previously analysed in the experimental section, the elastic modulus was measured for each loading cycle employing the ASTM D3039 methodology for the calculation of the chord modulus. As has been extensively reported in the literature both analytically and experimentally [30, 34–37], as matrix cracks initially develop the material becomes more compliant. In the case of step loading stiffness reduction will be observed when the loading threshold for transverse matrix cracking is exceeded. In this work, stiffness reduction is observed even from the second cycle, compared to the first. At the final cycle, the modulus has decreased by approximately 30 to 40 %. This stiffness degradation is primarily due to matrix cracking and the subsequent creation of ineffective stress transfer zones at the 0°/90° interface which trigger interlaminar failure. As the stress approaches the ultimate strength of the material, stiffness degradation becomes more prominent. Arguably, the observed stiffness loss may also be attributed to cumulative longitudinal fibre failure, but this would only be observed at the final loading stages. Figure 3a depicts the measured stiffness normalized by the initial stiffness for each cycle vs. the number of recorded AE hits. For the first stage of loading, AE hits are less than 100, but they increase for each successive step reaching almost 20,000 hits for the last. The stiffness loss vs. the number of hits curve falls rapidly in the first cycles and with decreased rate in the following cycles. In Fig. 3a logarithmic fitting function is employed to highlight the correlation.

In Fig. 3b, the number of AE hits vs. the sustained load is shown. Increasing load causes more damage for each step, which as expected, leads to higher acoustic emission activity for each consecutive cycle. As expected for any material, the increase of load is translated to an increase of crack initiation and propagation events; AE activity therefore is bound to increase in total for each step, including signals from matrix cracking and delamination

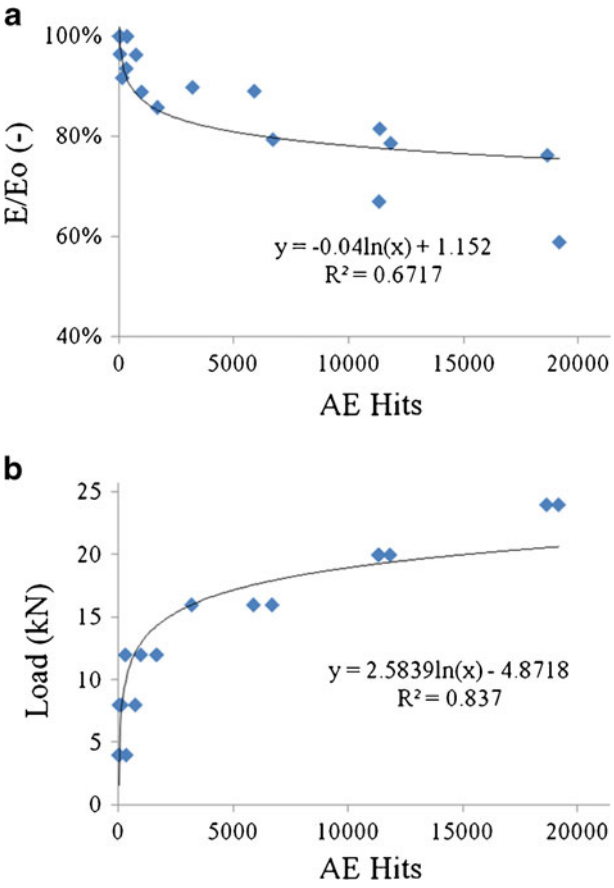

Fig. 3 Modulus degradation (**a**) and maximum sustained load (**b**) vs. number of AE hits. The entire data set in included in the figure

events. It is noteworthy, that the correlation between the sustained load and AE hits is much better than the correlation between the stiffness loss and the AE hits.

Apart from the number of emissions, a parameter that has been extensively used in AE monitoring is the AE energy [38]. It is usually presented in dimensionless form and is characteristic of the area under the rectified envelope of the signal waveform [39]. In this work, it is observed that the average energy of the signals for each loading step decreases with increasing load. In Fig. 4, the relative stiffness is depicted as a function of AE energy. Each value of AE energy stands for the average of the absolute energies of all the AE hits recorded for each step. As can be seen, the average energy exhibits a clearly decreasing trend with increasing load. This decrease relates to the mean energy of the recorded hits and not to the total energy which increases due to the increasing number of recorded hits directly attributed to the increasing total crack propagation rate with load. As was described in the Section 1 there is a succession of distinct damage modes that are activated during the loading of the cross ply composite: transverse cracking becomes saturated and triggers delaminations. It may be postulated that this well documented shift in damage type may lead to the decrease in average energy because delaminations emit signals with lower intensity than transverse cracks, and that the average energy released by an average delamination event is less than the energy of a cracking event. As should be noted, this observation was consistent

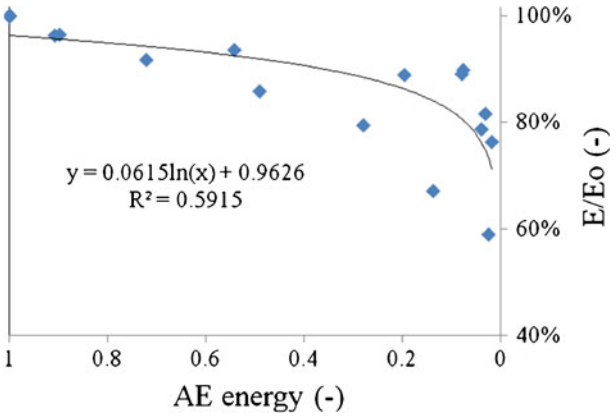

Fig. 4 Elastic modulus degradation vs. average AE energy for each step

for all tested specimens. As the cracking and the subsequent delamination process is directly relevant to the intelaminar shear strength between the 0° and the 90° plies, which is also directly relevant to the mode I (transverse cracking) versus mode II (delaminations) fracture toughness of the system and of course the fracture area for the respective modes. Higher interlaminar shear strength results to higher crack density and reduced delamination area. As in this approach no normalization to the fracture surfaces was feasible, it may be assumed that the behavior of the mean hit energy is directly related to the material and the geometry and may vary with interlaminar shear strength.

3.2 Connection with Damage Mode

The above observations enable the correlation between load or mechanical degradation and AE activity. However, it should be noted that (i) these correlations are highly system dependent and (ii) in order to be able to quantitatively assess damage, a large amount of experimental data is needed. Additionally to the above phenomenological correlations, more conclusions may be drawn on the fracture behavior by a more elaborate study of the characteristics of the recorded waveform.

As mentioned above, the shape of the waveform reveals information on the source crack motion that results in the corresponding signal. The initial part of the waveform is very characteristic and is examined by the rising angle of the signal (RA=Rise Time/Amplitude). In general, a shift from low to high RA values indicates transition from the tensile mode of crack to shear in different materials like concrete, rock and composites [11, 12, 19, 20, 25, 26]. As is mentioned in the literature, in some cases the information is examined by the "grade" which is the inverse of RA [11, 39]. In the case of step loading of cross ply laminates, as the load is monotonically increasing during each step, AE signals with higher RA are continuously recorded. This is indicatively shown in Fig. 5a and b for the 5th and 6th loading step respectively. For relatively low load (i.e. less than 10 kN) RA values are limited below 5 ms/V. As load increases, signals with higher RA start to be recorded reaching 100 ms/V when the load reaches its maximum. In contrast to the gradual built up of the RA prior to maximum load, after the load starts to descend, RA values return to the initial low level almost instantaneously. The same observation holds for Fig. 5b, where the RA values vs. time are shown for the consecutive loading step (maximum load 24 kN). In this case, the RA values reach almost 200 ms/V and are again quickly restored to the initial low level just after the load starts to descend, showing that the symmetry of the load curve is not followed by the AE activity.

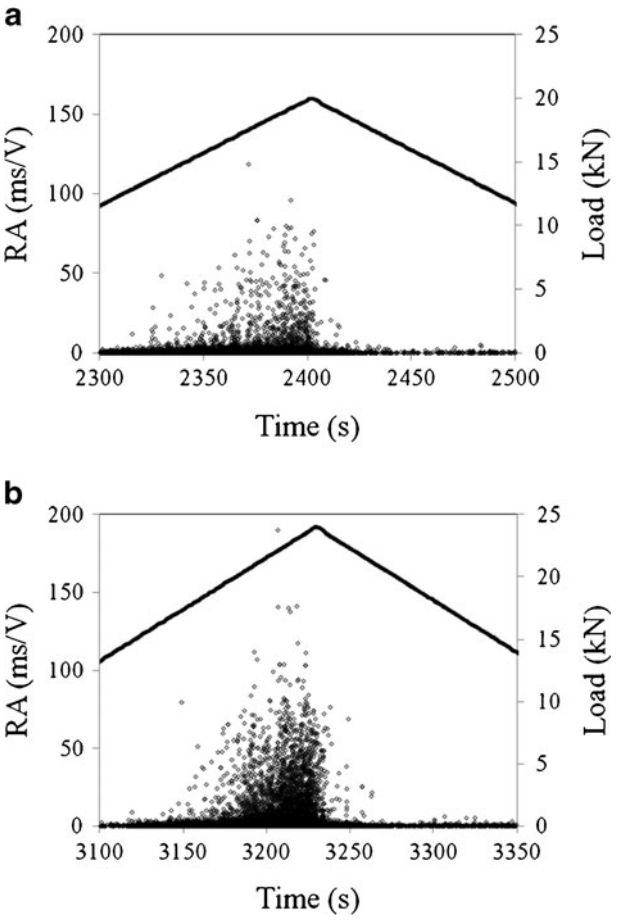

Fig. 5 Load and RA history for **a** the 5th step and **b** the 6th step for a typical specimen. The *solid line* represents the load and the *squares* the individual values of RA

It is interesting to discuss on the origin of this correlation between a mechanical property (elastic modulus) and a non-destructively measured parameter (acoustic emission RA). The connection and the reason behind this correlation is the sustained damage. The accumulation of damage in the form of cracking and delaminations is responsible for the measured degradation of modulus for each step. At the same time, when damage is being formed, the emitted acoustic waves strongly depend on the specific fracture mechanisms, and enable correlations between AE qualitative characteristics and modulus degradation.

Figure 6 shows the RA behavior for distinct loading steps. The RA of the increasing population of signals is shifted to higher levels, as the loading steps proceed; at the final step some signals exhibit RA close or higher than 200 ms/V (see Fig. 6). This increase can be considered indicative of the gradually increasing population of delamination events, which follow matrix cracking [40]. Indicative of the up shift of the RA is the average RA for the whole population of hits during each loading cycle. Figure 7a depicts the correlation between the sustained load and the mean RA value for each step The acoustic signature of the active damage mechanisms depends of the type of damage the mechanism is inducing and may be traced in the

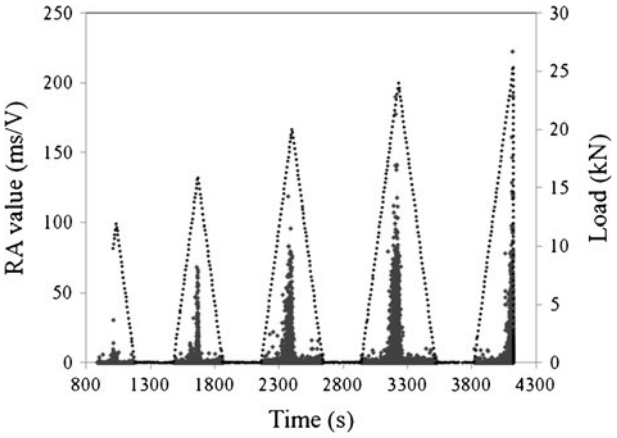

Fig. 6 RA and load history for five successive loading steps (step 6 is the final). The *solid line* represents the load and the *squares* the individual values of RA

characteristics of the acquired waveforms. In their turn, these are indicative of the dominant damage mode at any stage of loading of the structure. Moreover, the shift of RA can be well correlated to the degradation of elastic modulus. This is shown in Fig. 7b. For the first loading step, when the material operates on its original modulus, RA averages at values around 0.2 ms/V. As the modulus decreases for each successive step, average RA values increase reaching 3 ms/V for the last step when the stiffness is less than 50 % compared to that of the virgin material.

Another potentially useful correlation comes from the study of the central frequency of the signals of each successive step. Central frequency is defined as the centroid of the Fast Fourier Transform of the recorded waveforms and has been shown to be sensitive to damage in CFRP reinforced concrete slabs [41]. In the present study, due to the relatively broad bandwidth of the sensors' response, this feature potentially carries information directly related to the emitting source. For all specimens, the central frequency increases for each successive step. It starts at approximately 300 kHz and increases to 450 kHz for the last stage. This is quite strongly correlated to the elastic modulus, as seen in Fig. 8, allowing estimation of the mechanical degradation based on the frequency content of the AE waveforms. However, the explanation of the connection between the damage mode or the modulus of the material at that stage and central frequency is not straightforward. As is already mentioned in the Section 1, for macroscopically isotropic materials development of shear cracks emits AE signals with lower frequency than tensile [21–24]. In the specific case, though this transition is reasonable (matrix cracks to delaminations) the frequency content of the emissions is also related to the tension that the fibres. As is known, strings possess resonant frequencies that directly related to the mass, length, and tension of the string. As the load increases, the natural frequency of the fibres is elevated. Therefore, it is reasonable that any cracking incidences attributed to higher load will emit most of the energy in the natural frequency which is continuously increasing. In all cases, this distinction in the case of the studied cross ply laminate may be regarded as characteristic of different damage mechanisms which possess different acoustic signatures and become dominant at specific stages of the loading history.

3.3 Kaiser Effect

One of the most basic principles of acoustic emission is the "Kaiser" effect. According to Kaiser [42], no acoustic emission will be recorded by a material until the previous maximum

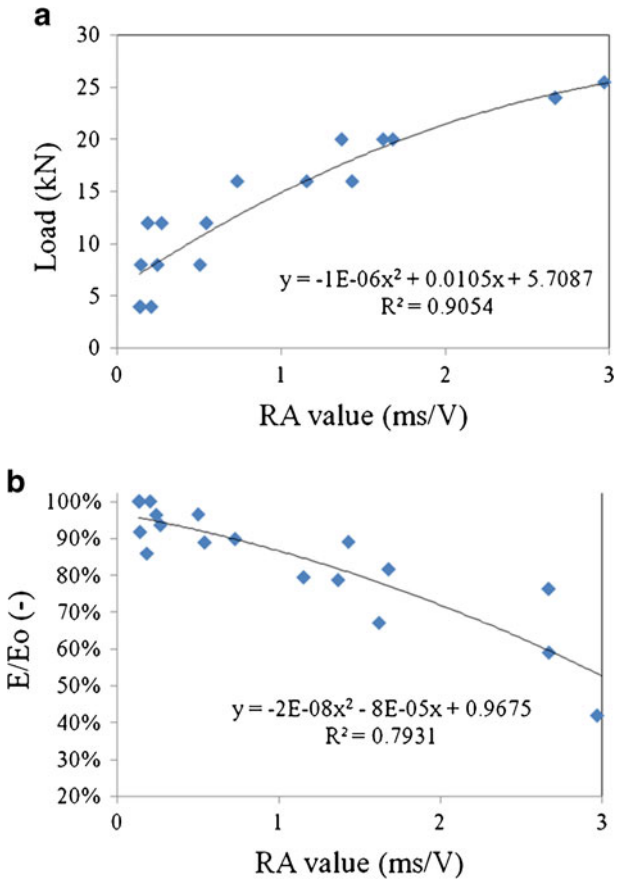

Fig. 7 Maximum sustained load (**a**) and stiffness loss (**b**) vs. mean RA value for all consecutive steps

load has been surpassed. This is because any damage owing to a specific load level is developed at the first loading. If the material is unloaded and loaded again, significant damage will start to propagate only after the load exceeds the previous maximum value. Materials that follow the "Kaiser" effect are considered quite intact, while if the load at the onset of AE is substantially lower than the previous maximum load, the material is

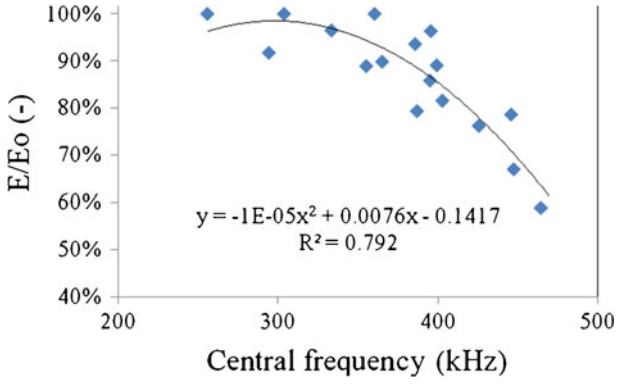

Fig. 8 Central frequency of AE vs. load

characterized as considerably damaged. Alternatively, this may be shown by the reduction in felicity ratio, or the ratio between the applied load at which the acoustic emission reappears during the next application of loading and the previous maximum applied load [43].

In the specific case, the Kaiser effect could be examined due to the successive incremental load steps that were applied to the material. In this discussion the focus will be on the AE events, or the pairs of hits that were almost simultaneously recorded by both sensors and therefore can be attributed to the same damage propagation incident. Figure 9a shows the number of events vs. time for each successive load step for one specimen. For the sake of presentation, in the figure the starting time of each cycle is translated to zero, so that the time is always reset to zero at the onset of each cycle. The first events are recorded during the 3rd cycle (with max. load 12 kN) until the time of 141 s, which is the time of maximum load. Thereafter, load decreases constantly until zero and starts to increase for the 4th step. During the 4th step, the first events are recorded some seconds later than the last events of the previous step and while the load has surpassed the previous maximum value. The events essentially stop after 200 s and for the 5th cycle they are recorded between 225 and 260 s. The events of the 6th cycle start at 283, again after the corresponding time of the previous step's last events and after the maximum load have been surpassed and last essentially up to

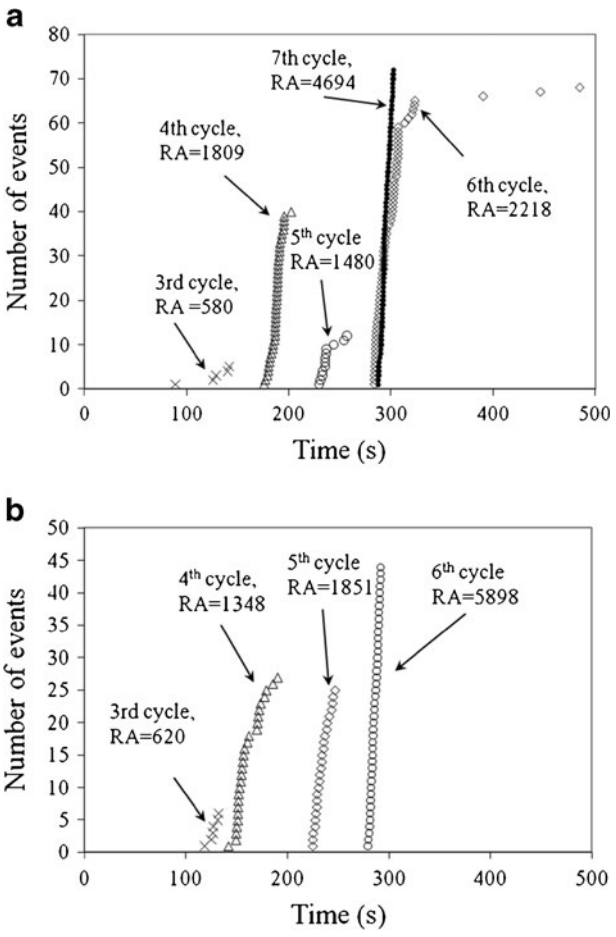

Fig. 9 **a** and **b** Cumulative AE events for successive loading cycles vs. time for two specimens. RA values are in μs/V

323 s while three more events are detected quite later for lower load. It is seen that the Kaiser effect holds up to this point and events are recorded after the previous maximum load has been surpassed. However, this trend is not repeated for the last (7th) cycle. There, the events start to occur at 287 s and the specimen fails at 302 s, with continuously recorded events. The events of this loading step do not show any trend of saturation, as was observed in the previous stages, which is connected to the nature of the events. There are distinct changes in the acoustic activity for the recorded events for the seventh cycle i.e. the early onset and the absence of a saturation stage. These may be attributed to the silencing of a previously dominant damage mechanism due to saturation and the domination of a damage entity which is interconnected or sequential to the previously dominant mechanism. This does not exclude the possibility that the latter mechanism was also active in the specimen during the previous loading cycles. This is consistent with the observation that transverse cracking is at some stage reaching saturation and other mechanisms become dominant. The events of the last stage could be attributed to damage entities other than transverse cracking such as delaminations or longitudinal fibre cracking, which initiate after the transverse cracking but continue to be active until the final failure of the material, unlike the matrix cracking that is led to a saturation level earlier. As should be mentioned, delaminations are more favoured to longitudinal fibre cracking as the onset of the event recording is observed very early, whereas longitudinal fibre cracking is expected to take place at higher strains.

On the same figure (Fig. 9a) one can see the corresponding RA value as an average for the number of events of each cycle. While the Kaiser effect holds, the RA is below 2,000 μs/V (until 5th cycle). After RA exceeds 2,000 μs/V (6th cycle), the Kaiser effect is not followed any more, the events start to occur earlier than the previous maximum load and the material fails recording events with RA close to 5,000 μs/V. As discussed in the previous section, this is indicative of a shift in the damage mode from tensile to shear, or from transverse cracking to shear failure, such as delamination.

Another example is depicted in Fig. 9b. In this case the behavior is similar, while the Kaiser effect can be observed until the final step, when the material is ruptured. In this case the events of the last (6th) step start to be recorded after the events of the previous cycle, which resulted in a RA value of less than 2,000 μs/V. This value of RA around the level of 2,000 μs/V could be discussed as a threshold for the observation of the Kaiser effect in the specific experimental conditions. In both cases, the rate of events at the last step seems constant until the final rupture of the material, which is reasonable since delaminations do not reach saturation like matrix cracks. It is reminded that as far as matrix cracks are concerned, a saturation level in the number of events is expected, depending on the materials' strength and the interlaminar shear strength. This behavior however, is being masked by the propagation of delaminations which do not reach saturation until failure, seen by the constant rate of events occurring at the final step of the materials (see Fig. 9a and b). This leads to a discussion about the Kaiser effect and whether it should be examined for the material as a whole or more likely for the different fracture mechanisms inside the material. It is reasonable that in order for new matrix cracks to open up, the stress should be higher than the previously reached. However, for the delaminations it is not necessarily the same. The tip of the delamination acts as a stress concentration point, where the rate of stress transfer or the shear stress reaches its maximum value. The axial stress concentration may drive the crack through the 0° layer, or the shear stress may deflect it at the interlaminar area if the interlaminar shear strength is reached. As the interlaminar shear is a function of the transfer length, delaminations are expected to be activated every time a transverse crack is formed and progress with the application of load. In this respect, they are always an active damage mechanism, even before the previous maximum externally applied load has been reached.

4 Conclusions

In this study the acoustic emission behavior of GFRP cross-ply laminates is examined under triangular step tensile loading. AE activity originates from the cracking incidences within the material. The total number of AE activity is strongly related to the sustained load, while it is also well related to the degradation of the modulus for each successive loading step. Acoustic emission parameters are used to correlate with mechanical properties during fracturing. Parameters like the AE energy and RA value are found to be sensitive to the failure mode and accumulation, since they gradually shift as the dominant fracture mechanism changes from matrix cracking to delaminations. Therefore, they can be studied as damage indices associated to the damage conversion in cross ply composites with increasing load. Furthermore, due to the different mechanisms that may act successively, simultaneously or overlapping, the Kaiser effect is discussed not as a single phenomenon characteristic of the material, but as characteristic of each fracture mechanism.

References

1. Nairn, J., Hu, S.: Matrix microcracking. Elsevier, (1994)
2. Guild, F.J., Vrellos, N., Drinkwater, B.W., Balhi, N., Ogin, S.L., Smith, P.A.: Intra-laminar cracking in CFRP laminates: observations and modelling. J. Mater. Sci. **41**(20), 6599–6609 (2006)
3. Wang, H., Ogin, S.L., Thorne, A.M., Reed, G.T.: Interaction between optical fibre sensors and matrix cracks in cross-ply GFRP laminates. Part 2: crack detection. Compos. Sci. Technol. **66**(13), 2367–2378 (2006)
4. Talreja, R.: Fatigue of composite materials. Technomic Pub. Co., (1987)
5. Mix, P.E.: Introduction. In: Introduction to Nondestructive Testing, pp. 1–13. John Wiley & Sons, Inc., (2005)
6. Yun, H.D., Choi, W.C., Seo, S.Y.: Acoustic emission activities and damage evaluation of reinforced concrete beams strengthened with CFRP sheets. NDT E Int. **43**(7), 615–628 (2010)
7. Grosse, C.U., Ohtsu, M.: Acoustic emission testing. Springer, (2008)
8. Kostopoulos, V., Loutas, T.H., Kontsos, A., Sotiriadis, G., Pappas, Y.Z.: On the identification of the failure mechanisms in oxide/oxide composites using acoustic emission. NDT E Int. **36**(8), 571–580 (2003)
9. Loutas, T.H., Kostopoulos, V.: Health monitoring of carbon/carbon, woven reinforced composites. Damage assessment by using advanced signal processing techniques. Part I: acoustic emission monitoring and damage mechanisms evolution. Compos. Sci. Technol. **69**(2), 265–272 (2009)
10. Vavouliotis, A., Karapappas, P., Loutas, T., Voyatzi, T., Paipetis, A., Kostopoulos, V.: Multistage fatigue life monitoring on carbon fibre reinforced polymers enhanced with multiwall carbon nanotubes. Plast. Rubber Compos. **38**(2–4), 124–130 (2009)
11. Aggelis, D.G., Shiotani, T., Momoki, S., Hirama, A.: Combined stress wave techniques for damage characterization of composite concrete elements. Am. Concr. Inst. Mater. J. **107**(5), 469–473 (2009)
12. Overgaard, L.C.T., Lund, E., Camanho, P.P.: A methodology for the structural analysis of composite wind turbine blades under geometric and material induced instabilities. Comput. Struct. **88**(19–20), 1092–1109 (2010)
13. Schechinger, B., Vogel, T.: Acoustic emission for monitoring a reinforced concrete beam subject to four-point-bending. Construct. Build. Mater. **21**(3), 483–490 (2007)
14. Tobias, A.: Acoustic-emission source location in two dimensions by an array of three sensors. Non-destruct. Test. **9**(1), 9–12 (1976). doi:10.1016/0029-1021(76)90027-x
15. Caprino, G., Lopresto, V., Leone, C., Papa, I.: Acoustic emission source location in unidirectional carbon-fiber-reinforced plastic plates with virtually trained artificial neural networks. J. Appl. Polym. Sci. **122**(6), 3506–3513 (2011). doi:10.1002/app. 34758
16. Jeong, H., Jang, Y.-S.: Wavelet analysis of plate wave propagation in composite laminates. Compos. Struct. **49**(4), 443–450 (2000). doi:10.1016/s0263-8223(00)00079-9
17. Kundu, T., Das, S., Martin, S.A., Jata, K.V.: Locating point of impact in anisotropic fiber reinforced composite plates. Ultrasonics **48**(3), 193–201 (2008). doi:10.1016/j.ultras.2007.12.001

18. Su, Y., Liu, X., Li, D., Wang, X., Zhang, Y.: Research on impact localization in composite materials using array signal processing and Lamb wave. In, vol. 304, pp. 65–72. (2011)
19. Aggelis, D.G., Soulioti, D.V., Sapouridis, N., Barkoula, N.M., Paipetis, A.S., Matikas, T.E.: Acoustic emission characterization of the fracture process in fibre reinforced concrete. Construct. Build. Mater. **25** (11), 4126–4131 (2011)
20. Aggelis, D.G., Matikas, T.E., Shiotani, T. (eds.): Advanced acoustic techniques for health monitoring of concrete structures. Middleton Publishing Inc., Seoul (2010)
21. Ohtsu, M.: Recommendation of RILEM TC 212-ACD: acoustic emission and related NDE techniques for crack detection and damage evaluation in concrete: test method for classification of active cracks in concrete structures by acoustic emission. Mater. Struct./Mater. Constr. **43**(9), 1187–1189 (2010)
22. Shiotani, T.: Evaluation of long-term stability for rock slope by means of acoustic emission technique. NDT E Int. **39**(3), 217–228 (2006)
23. Lu, Y., Li, Z., Liao, W.I.: Damage monitoring of reinforced concrete frames under seismic loading using cement-based piezoelectric sensor. Mater. Struct./Mater. Constr. **44**(7), 1273–1285 (2011)
24. Ohno, K., Ohtsu, M.: Crack classification in concrete based on acoustic emission. Construct. Build. Mater. **24**(12), 2339–2346 (2010)
25. de Oliveira, R., Marques, A.T.: Health monitoring of FRP using acoustic emission and artificial neural networks. Comput. Struct. **86**(3–5), 367–373 (2008)
26. Kostopoulos, V., Tsotra, P., Karapappas, P., Tsantzalis, S., Vavouliotis, A., Loutas, T.H., Paipetis, A., Friedrich, K., Tanimoto, T.: Mode I interlaminar fracture of CNF or/and PZT doped CFRPs via acoustic emission monitoring. Compos. Sci. Technol. **67**(5), 822–828 (2007)
27. Scholey, J.J., Wilcox, P.D., Wisnom, M.R., Friswell, M.I.: Quantitative experimental measurements of matrix cracking and delamination using acoustic emission. Compos. A: Appl. Sci. Manuf. **41**(5), 612–623 (2010)
28. Gorman, M.R., Prosser, W.H.: AE Source Orientation by plate wave analysis. J. Acoust. Emission **9**(4), 283–288 (1990)
29. Venturini Autieri, M.R., Dulieu-Barton, J.M.: Initial studies for AE characterisation of damage in composite materials. In, vol. 13-14, pp. 273-280. (2006)
30. Katerelos, D.T.G., Paipetis, A., Loutas, T., Sotiriadis, G., Kostopoulos, V., Ogin, S.L.: In situ damage monitoring of cross-ply laminates using acoustic emission. Plast. Rubber Compos. **38**(6), 229–234 (2009)
31. http://www.pacndt.com/index.aspx?go=products&focus=/sensors/miniature.htm
32. Ramesh, C., Ragesh, H., Arumugam, V., Stanley, A.: Effect of hydrolytic ageing on Kevlar/polyester using acoustic emission monitoring. J. Nondestruct. Eval. **31**(2), 140–147 (2012). doi:10.1007/s10921-012-0129-9
33. de Groot, P.J., Wijnen, P.A.M., Janssen, R.B.F.: Real-time frequency determination of acoustic emission for different fracture mechanisms in carbon/epoxy composites. Compos. Sci. Technol. **55**(4), 405–412 (1995)
34. Aggelis, D.G., Barkoula, N.M., Matikas, T.E., Paipetis, A.S.: Acoustic structural health monitoring of composite materials : Damage identification and evaluation in cross ply laminates using acoustic emission and ultrasonics. Compos. Sci. Technol. (2011)
35. Hashin, Z., Rosen, B.W.: Macro-residual strains due to cyclic loading of composites. Mech. Compos. Mater. Struct. **6**(3), 257–266 (1999)
36. Krasnikovs, A., Varna, J.: Transverse cracks in cross-ply laminates. 1. Stress analysis. Mech. Compos. Mater. **33**(6), 565–582 (1997)
37. Varna, J., Berglund, L.A.: Thermo-elastic properties of composite laminates with transverse cracks. J. Compos. Technol. Res. **16**(1), 77–87 (1994)
38. Kostopoulos, V., Karapappas, P., Loutas, T., Vavouliotis, A., Paipetis, A., Tsotra, P.: Interlaminar fracture toughness of carbon fibre-reinforced polymer laminates with nano- and micro-fillers. Strain **47**(SUPPL. 1), e269–e282 (2011)
39. Anastassopoulos, A.A., Philippidis, T.P.: Clustering methodology for the evaluation of AE from composites. J. Acoust. Emission **13**, 11–22 (1995)
40. Aggelis, D.G., Barkoula, N.M., Matikas, T.E., Paipetis, A.S.: Acoustic emission monitoring of degradation of cross ply laminates. J. Acoust. Soc. Am. **127**(6), EL246–EL251 (2010). doi:10.1121/1.3425752
41. Degala, S., Rizzo, P., Ramanathan, K., Harries, K.A.: Acoustic emission monitoring of CFRP reinforced concrete slabs. Construct. Build. Mater. **23**(5), 2016–2026 (2009)
42. Kaiser, J.: Results and Conclusions from Measurements of Sound in Metallic Materials under Tensile Stress. Technische Hochshule (1950)
43. Li, C., Nordlund, E.: Experimental verification of the Kaiser effect in rocks. Rock Mech. Rock. Eng. **26** (4), 333–351 (1993)